
**MODELING THE CORONA AND SOLAR WIND
USING ADAPT MAPS THAT INCLUDE FAR-SIDE
OBSERVATIONS
(Postprint)**

C. Nick Arge, et al.

01 November 2013

Interim Report

APPROVED FOR PUBLIC RELEASE; DISTRIBUTION IS UNLIMITED.



**AIR FORCE RESEARCH LABORATORY
Space Vehicles Directorate
3550 Aberdeen Ave SE
AIR FORCE MATERIEL COMMAND
KIRTLAND AIR FORCE BASE, NM 87117-5776**

DTIC COPY

NOTICE AND SIGNATURE PAGE

Using Government drawings, specifications, or other data included in this document for any purpose other than Government procurement does not in any way obligate the U.S. Government. The fact that the Government formulated or supplied the drawings, specifications, or other data does not license the holder or any other person or corporation; or convey any rights or permission to manufacture, use, or sell any patented invention that may relate to them.

This report was cleared for public release by the 377 ABW Public Affairs Office and is available to the general public, including foreign nationals. Copies may be obtained from the Defense Technical Information Center (DTIC) (<http://www.dtic.mil>).

AFRL-RV-PS-TR-2014-0086 HAS BEEN REVIEWED AND IS APPROVED FOR PUBLICATION IN ACCORDANCE WITH ASSIGNED DISTRIBUTION STATEMENT.

//SIGNED//

Dr. Charles N. Arge
Program Manager, AFRL/RVBXS

//SIGNED//

Edward J. Masterson, Colonel, USAF
Chief, Battlespace Environment Division

This report is published in the interest of scientific and technical information exchange, and its publication does not constitute the Government's approval or disapproval of its ideas or findings.

REPORT DOCUMENTATION PAGE

Form Approved
OMB No. 0704-0188

Public reporting burden for this collection of information is estimated to average 1 hour per response, including the time for reviewing instructions, searching existing data sources, gathering and maintaining the data needed, and completing and reviewing this collection of information. Send comments regarding this burden estimate or any other aspect of this collection of information, including suggestions for reducing this burden to Department of Defense, Washington Headquarters Services, Directorate for Information Operations and Reports (0704-0188), 1215 Jefferson Davis Highway, Suite 1204, Arlington, VA 22202-4302. Respondents should be aware that notwithstanding any other provision of law, no person shall be subject to any penalty for failing to comply with a collection of information if it does not display a currently valid OMB control number. **PLEASE DO NOT RETURN YOUR FORM TO THE ABOVE ADDRESS.**

1. REPORT DATE (DD-MM-YYYY) 01-11-2013		2. REPORT TYPE Interim Report		3. DATES COVERED (From - To) 01 Nov 2011 to 31 Oct 2013	
4. TITLE AND SUBTITLE Modeling the Corona and Solar Wind using ADAPT Maps that Include Far-Side Observations (Postprint)				5a. CONTRACT NUMBER	
				5b. GRANT NUMBER	
				5c. PROGRAM ELEMENT NUMBER 61102F	
6. AUTHOR(S) C. Nick Arge, Carl J. Henney, Irene Gonzalez Hernandez ² , W. Alex Toussaint ² , Josef Koller ³ , and Humberto C. Godinez ³				5d. PROJECT NUMBER 2301	
				5e. TASK NUMBER PPM00005114	
				5f. WORK UNIT NUMBER EF004379	
7. PERFORMING ORGANIZATION NAME(S) AND ADDRESS(ES) Air Force Research Laboratory Space Vehicles Directorate 3550 Aberdeen Avenue SE Kirtland AFB, NM 87117-5776				8. PERFORMING ORGANIZATION REPORT NUMBER AFRL-RV-PS-TR-2014-0086	
				² National Solar Observatory 950 N Cherry Avenue Tucson, AZ 85719	
				³ Los Alamos National Laboratory PO Box 1663 Los Alamos, NM 87545	
9. SPONSORING / MONITORING AGENCY NAME(S) AND ADDRESS(ES)				10. SPONSOR/MONITOR'S ACRONYM(S) AFRL/RVBXS	
				11. SPONSOR/MONITOR'S REPORT NUMBER(S)	
12. DISTRIBUTION / AVAILABILITY STATEMENT Approved for public release; distribution is unlimited. (377ABW-2012-1348 dtd 11 Oct 2012)					
13. SUPPLEMENTARY NOTES Accepted for publication in Solar Wind 13, AIP Conference Series: 01 June 2013. Government Purpose Rights.					
14. ABSTRACT As the primary input to nearly all coronal and solar wind models, global estimates of the solar photospheric magnetic field distribution are critical for reliable modeling of the corona and heliosphere. Over the last several years the Air Force Research Laboratory (AFRL), in collaboration with Los Alamos National Laboratory (LANL) and the National Solar Observatory (NSO), has developed a model that produces more realistic estimates of the instantaneous global photospheric magnetic field distribution than those provided by traditional photospheric field synoptic maps. The Air Force Data Assimilative Photospheric flux Transport (ADAPT) model is a photospheric flux transport model, originally developed at NSO, that makes use of data assimilation methodologies developed at LANL. The flux transport model evolves the observed solar magnetic flux using relatively well understood transport processes when measurements are not available and then updates the modeled flux with new observations using data assimilation methods that rigorously take into account model and observational uncertainties. ADAPT originally only made use of Earth-side magnetograms, but the code has now been modified to assimilate helioseismic far-side active region data such as those available from the Global Oscillation Network Group. As a preliminary test, a helioseismically detected active region that first emerged on the far-side of the Sun in early July 2010 is incorporated into maps produced by ADAPT and then used in the Wang-Sheeley-Arge (WSA) model to simulate the corona and solar wind. The WSA model results, with and without far-side data included in the ADAPT global maps, are compared here with coronal EUV and in situ solar wind observations available from STEREO. We find that the observed and modeled values are in better agreement when including the far-side detection.					
15. SUBJECT TERMS Solar Wind; Coronal Holes; Helioseismic far-side; Magnetic Flux Transport					
16. SECURITY CLASSIFICATION OF:			17. LIMITATION OF ABSTRACT Unlimited	18. NUMBER OF PAGES 10	19a. NAME OF RESPONSIBLE PERSON Dr. C. Nick Arge
a. REPORT Unclassified	b. ABSTRACT Unclassified	c. THIS PAGE Unclassified			19b. TELEPHONE NUMBER (include area code)

This page is intentionally left blank.

Modeling the Corona and Solar Wind using ADAPT Maps that Include Far-Side Observations

C. Nick Arge^{*}, Carl J. Henney^{*}, Irene Gonzalez Hernandez[†], W. Alex Toussaint[†], Josef Koller^{**} and Humberto C. Godinez^{**}

^{*}*AFRL/Space Vehicles Directorate, Kirtland AFB, NM, USA*

[†]*National Solar Observatory, Tucson, AZ, USA*

^{**}*Los Alamos National Laboratory, Los Alamos, NM, USA*

Abstract. As the primary input to nearly all coronal and solar wind models, global estimates of the solar photospheric magnetic field distribution are critical for reliable modeling of the corona and heliosphere. Over the last several years the Air Force Research Laboratory (AFRL), in collaboration with Los Alamos National Laboratory (LANL) and the National Solar Observatory (NSO), has developed a model that produces more realistic estimates of the instantaneous global photospheric magnetic field distribution than those provided by traditional photospheric field synoptic maps. The Air Force Data Assimilative Photospheric flux Transport (ADAPT) model is a photospheric flux transport model, originally developed at NSO, that makes use of data assimilation methodologies developed at LANL. The flux transport model evolves the observed solar magnetic flux using relatively well understood transport processes when measurements are not available and then updates the modeled flux with new observations using data assimilation methods that rigorously take into account model and observational uncertainties. ADAPT originally only made use of Earth-side magnetograms, but the code has now been modified to assimilate helioseismic far-side active region data such as those available from the Global Oscillation Network Group. As a preliminary test, a helioseismically detected active region that first emerged on the far-side of the Sun in early July 2010 is incorporated into maps produced by ADAPT and then used in the Wang-Sheeley-Arge (WSA) model to simulate the corona and solar wind. The WSA model results, with and without far-side data included in the ADAPT global maps, are compared here with coronal EUV and in situ solar wind observations available from STEREO. We find that the observed and modeled values are in better agreement when including the far-side detection.

Keywords: Solar Wind; Coronal Holes; Helioseismic far-side; Magnetic Flux Transport

PACS: 96.50.Ci; 96.60.pc; 96.60.Hv; 96.60.Ly

INTRODUCTION

Solar corona and wind models, e.g., the Wang-Sheeley-Arge (WSA) model [1, 2, 3], require an estimate of the instantaneous global solar magnetic field as input for the inner boundary condition. The Air Force Research Laboratory, in collaboration LANL and NSO, is developing ADAPT (Air Force Data Assimilative Photospheric Flux Transport; [4, 5]) to produce realistic global photospheric magnetic field maps. The ADAPT model utilizes a modified version of the Worden and Harvey flux transport model [6] to best approximate the instantaneous magnetic flux distribution using well known surface flow patterns (e.g., differential rotation) and supergranular diffusion.

The global maps generated for this study were created with line-of-sight full-disk magnetogram data from the Vector Spectromagnetograph (VSM; [7]). VSM magnetograms are recorded at a cadence of approximately one per day during good weather. Each time a new magnetogram is available from a selected source ADAPT generates a new global map. If no data are available from a source for more than ~ 24 hours, the model generates a

daily map by default.

The ADAPT model code has recently been modified to assimilate far-side active region data. The detection of large active regions on the far-side of the Sun is possible using the helioseismic acoustic holography technique [e.g., 8]. This unique approach provides the approximate location, size, and magnetic strength of new field emergence. In addition to improving estimates of the global magnetic field distribution, the inclusion of far-side data into ADAPT maps allows for the increase of the model variance to facilitate rapid assimilation of new flux when observed at the limb.

Without helioseismic far-side detections, the first indication of a new region that emerged on the far-side of the sun is its appearance on the east limb where observational errors are typically much higher than those of the model. This is especially true for active regions, which naturally have larger variance than weak field areas. Large observational errors at the limb arise from foreshortening and the canopy effect, along with a variable horizontal magnetic signal that increases towards the observed limb [9]. From a data assimilative perspective, model field values are thus usually given more

weight at the limb than observations. This is a problem for a new active region that emerges in a previously weak field area on the solar far-side, for when it first arrives at the limb, the near-side observations of the region are initially weighted very low by the data assimilation. However, if the far-side data are assimilated before it arrives at the limb, the near-side observations now have greater weight because the model variance is also increased for that region.

INCORPORATING FAR-SIDE DATA

Since the helioseismic inference of the field strength on the far-side does not discern polarity information, known statistical and cycle properties for active regions are utilized (i.e., Hale’s and Joy’s rules) to estimate the polarity order and orientation. For example, Hale’s law correctly predicts polarity $\sim 90\%$ of the time [10]. The far-side signals used here were parameterized in terms of photospheric magnetic field strength [11] as observed by the Global Oscillation Network (GONG). Since the ADAPT maps for this study use VSM magnetograms, an additional scaling factor of 1.4 is applied to the far-side values to account for a derived difference between GONG & VSM magnetograms before merging the signals into the ADAPT maps.

To estimate the polarity distribution of the far-side active region, the field strength signal is split east-west, to nearest equal sums, making one half negative (depending on hemisphere and current cycle), then scaled so that the mean flux of the active region sums to zero. When merged with the ADAPT map, the mean of the replaced pixels is preserved to avoid introducing a monopole to the global map. As a check of the estimated field strength and location, the merged and evolved far-side signal within ADAPT maps were used to model the solar radio flux at 2.8 GHz (i.e., 10.7 cm) following Henney et al. [12]. We found that the inclusion of the far-side signal resulted in predicted values in excellent agreement with the observed radio flux, providing preliminary validation of the calibration of the original far-side area, location, and field strength values. The far-side merged ADAPT maps were then utilized as input to WSA to study the difference between solutions with and without the new active region field strength and polarity estimates included, as discussed in the following section.

WSA WITH ADAPT FAR-SIDE MAPS

Two sets of daily photospheric magnetic field maps spanning two solar rotations (i.e., Carrington rotations (CR) 2098 & 2099, mid-June through mid-August, 2010) were generated using the ADAPT model. The first set

includes the far-side observation of the active region AR11087, while the second is without the far-side data. Each ADAPT ensemble is comprised of 16 individual realizations all of which have different flux transport parameters (e.g., meridional flow rates). These two sets of maps were used as input to the WSA model to produce both coronal and solar wind solutions. Figure 1 illustrates two ADAPT photospheric magnetic field maps (a & b) from July 1, 2010, the day the far-side active region data was merged.

Figure 1a exhibits the original ADAPT map without far-side data, while Figure 1b shows the ADAPT map with the far-side active region included. The red crosses in both figures correspond to the sub-STEREO B positions. Coincidentally, the active region was first detected helioseismically when it was located almost exactly on the opposite side of the sun. Since the central meridian, as viewed from the Earth, is routinely positioned at the center of the ADAPT maps, the new active region appears split in half in Figure 1b (delineated by the circles), with the negative (positive) polarity portion of the region appearing on the left (right) side of the map.

The same global STEREO EUVI map (i.e., the green images) corresponding to July 1, 2010 is shown in both Figures 1c & 1d. The map was constructed from the individual STEREO A & B EUVI disk images from that particular day. The global EUVI maps are co-aligned with the photospheric field maps displayed in Figures 1a and 1b, except that the longitudes displayed on the horizontal axes of these figures indicate distance from the central meridian (i.e., longitude 153° in Carrington coordinates) with east/westward being negative/positive. Overplotted on these two EUVI maps are white contours depicting WSA coronal holes predictions based on using the two ADAPT maps seen in Figures 1a & 1b as input to the model.

The agreement between the observed coronal holes (primarily the dark regions in the EUVI map) and that determined by WSA is reasonably good. The main areas of apparent discrepancy occur near the limbs of the individual EUVI disk images where line-of-site effects become important (e.g., near the poles), and the WSA predicted southern coronal hole extension positioned at 30° east of the central meridian (i.e., -30° in the EUVI plots). The area of interest, circled in red in Figure 1c, is where three small coronal holes are predicted. In particular, the rightward-most coronal hole within the circle is positioned right on top of a small area with very bright EUV emission. This bright region is associated with the negative polarity of the active region located at $\sim 305^\circ$ longitude and $\sim 25^\circ$ latitude. This small hole is almost certainly not real, as coronal holes are usually dark in EUV, and it is not predicted by WSA when the large far-side active region is included in the ADAPT model (as illustrated in Figure 1d).

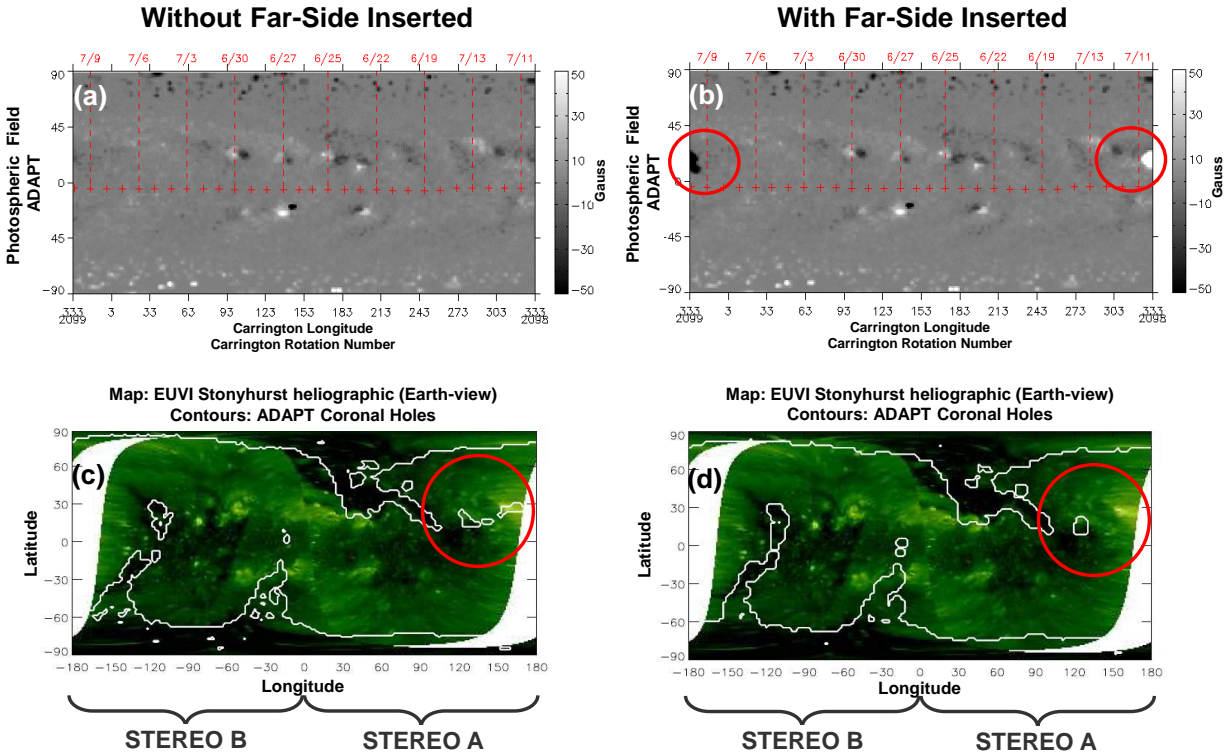


FIGURE 1. ADAPT photospheric magnetic field without far-side active region included (a) and with the far-side active region included (b) shown in upper row. The comparison of global STEREO EUVI map (green image) and WSA coronal hole predictions (white contours) rendered in (c) and (d) were obtained using (a) and (b), respectively, as inputs to the WSA model. Note that the small coronal hole positioned on top of the bright area of EUV emission (circled in red) in (c) has disappeared in (d).

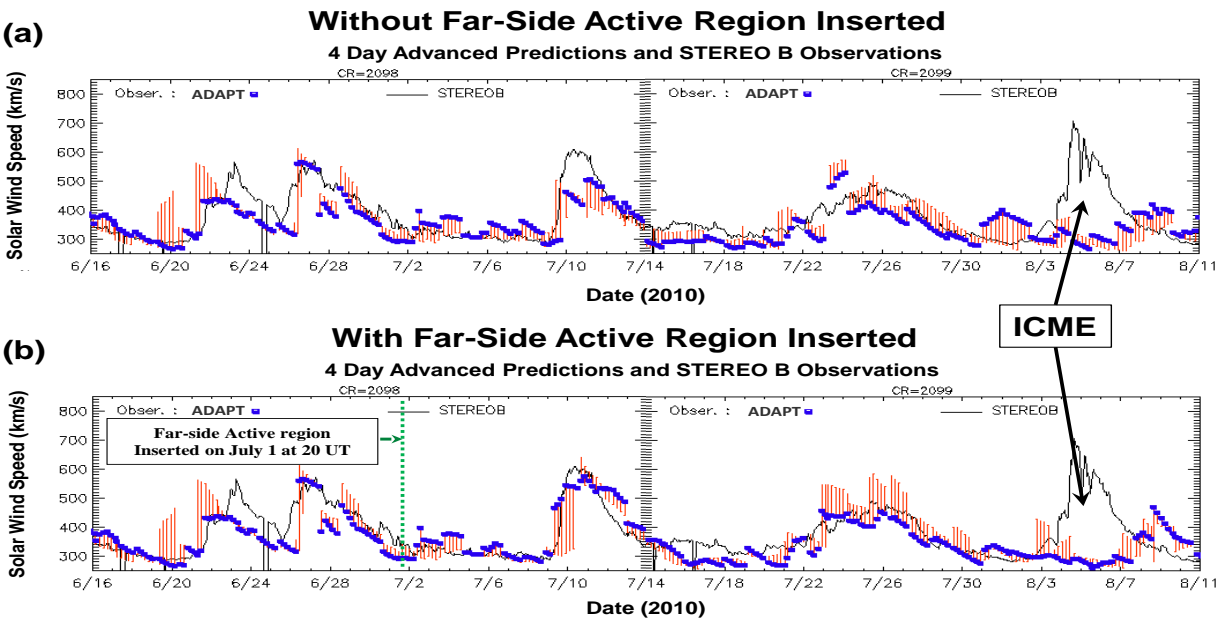


FIGURE 2. Solar wind speed observations from STEREO B (black solid lines) vs. WSA predictions (blue dots) using daily ADAPT maps without the far-side active region included (a). The lower time series (b) is the same as (a) except now using ADAPT maps with the far-side active region included.

Figure 2 features a comparison between the WSA predicted solar wind speed (blue dots) at the position of STEREO B and the in situ observations (solid black line) from that spacecraft over the time interval CR2098-2099. Figure 2a compares model predictions and STEREO B observations when the far-side active region is not included in the ADAPT maps, while Figure 2b demonstrates the comparison when it is included. The red vertical bars indicate the range over which WSA solar wind speed predictions vary over the span (in latitude) of one cell on the grid. In both cases the agreement between model predictions and observations is quite good. The only major discrepancy found is for the interplanetary coronal mass ejection (ICME) that arrived at STEREO B on August 4, 2010. Since WSA only predicts the slowly varying background solar wind, it is not expected to capture ICMEs, however, improvements in the modeled background wind using ADAPT is key to accurately modeling ICME propagation (see [13]).

Comparing the results highlighted in Figures 2a & 2b, note that the predictions in both are identical to each other until about July 6, 2010. This is true even though the far-side active region was assimilated into the ADAPT maps on July 1. This makes sense physically because it takes slow wind traveling at ~ 300 km/s about 5 days to reach 1AU. After July 6, the two solar wind prediction time series begin to differ noticeably from each other with those that include the far-side active region having better overall agreement with observations, especially for the high speed stream recorded by STEREO B on July 10. The structure of the coronal hole producing this stream changed when the active region was included.

To create the set of ADAPT maps that includes the July 1 helioseismically detected far-side active region, the ADAPT map from June 30 was evolved 24 hours and then merged with the far-side data as discussed in the previous section. Once the far-side active region rotated onto the visible side of Sun, the near-side observation of it is assimilated into the ADAPT maps. By July 10, one would expect the two sets of ADAPTS maps to resume being identical to each other and thus also produce identical solar wind speed predictions. After merging the far-side data, however, the new ADAPT model run is driven by a new set of randomly varying supergranular flows. So the ADAPT run with the far-side active region also evolves with a diverging supergranulation pattern. Starting on July 1, the two sets of maps thus begin to differ from one another because of different supergranulation flows and the far-side data. The differences in the two sets of solar wind predictions after the far-side active region moved onto the visible side of the disk is primarily due to the differing supergranulation patterns and not the result of the inclusion of the far-side active region. Differing supergranular flow patterns therefore clearly produce small, but noticeable, differences in the results.

CONCLUSION

The ADAPT model has been modified so that it can now merge helioseismically inferred far-side active data with global magnetic field maps. As a preliminary study of the far-side emergence of AR11087 (on July 1, 2010), we find that the observed and modeled values, i.e., coronal holes and solar wind velocity, are in better agreement when driven with maps including the far-side detection. Comparisons between STEREO observed coronal holes and STEREO B solar wind velocities highlight the improvement when including far-side data. Further work is needed to better understand how to represent the far-side polarity distribution and how the selected morphologies affect corona and solar wind results.

ACKNOWLEDGMENTS

The ADAPT software used here was developed with support by a grant from the AFOSR (Air Force Office of Scientific Research). The National Solar Observatory (NSO) data used for this work are produced cooperatively by National Science Foundation and the NSO.

REFERENCES

1. Arge, C. N. & Pizzo, V. J., *J. Geophys. Res.*, **105**, 10465 (2000).
2. Arge, C. N., Odstrcil, D., Pizzo, V. J., & Mayer, L. R., edited by M. Velli, R. Bruno, F. Malara, & B. Bucci, in *Solar Wind Ten*, **679**, 190 (2003).
3. Arge, C. N., Luhmann, J. G., Odstrcil, D., Schrijver, C. J., & Li, Y., *J. of Atmos. & Solar-Terr. Phys.*, **66**, 1295 (2004).
4. Arge, C. N., Henney, C. J., Koller, J., Compeau, C. R., Young, S., MacKenzie, D., Fay, A., & Harvey, J. W., *Twelfth International Solar Wind Conference*, **1216**, 343 (2010).
5. Arge, C. N., Henney, C. J., Koller, J., Toussaint, W. A., Harvey, J. W., & Young, S., in 5th International Conference of Numerical Modeling of Space Plasma Flows (ASTRONUM 2010), edited by N. V. Pogorelov, E. Audit, & G. P. Zank, *ASP Conf. Ser.*, **444**, 99 (2011).
6. Worden, J. & Harvey, J., *Solar Phys.*, **195**, 247-268 (2000).
7. Henney, C. J., Keller, C. U., Harvey, J. W., Georgoulis, M. K., Hadder, N. L., Norton, A. A., Raouafi, N.-E., & Toussaint, R. M., in *Solar Polarization 5: In Honor of Jan Stenflo*, edited by S. V. Berdyugina, K. N. Nagendra, & R. Ramelli, *ASP Conf. Ser.*, **405**, 47 (2009).
8. Lindsey, C. & Braun, D. C., *Astrophys. J.*, **485**, 895 (1997).
9. Harvey, J. W., Branston, D., Henney, C. J., Keller, C. U., & SOLIS & GONG Teams, *Astrophys. J.*, **659**, L177 (2007).
10. Li, J. & Ulrich, R., *Astrophys. J.*, **758**, 115 (2012).
11. González Hernández, I., Hill, F., & Lindsey, C., *Astrophys. J.*, **669**, 1382 (2007).
12. Henney, C. J., Toussaint, W. A., White, S. M., & Arge, C. N., *Space Weather*, **10**, 2011 (2012).
13. Lee, C. O., Arge, C. N., Odstrcil, D., Millward, G., Pizzo, V., Quinn, J. M., & Henney, C. J., *Solar Phys.*, **79** (2012).

DISTRIBUTION LIST

DTIC/OCP 8725 John J. Kingman Rd, Suite 0944 Ft Belvoir, VA 22060-6218	1 cy
AFRL/RVIL Kirtland AFB, NM 87117-5776	2 cys
Official Record Copy AFRL/RVBXS/Dr. Charles N. Arge	1 cy

This page is intentionally left blank.